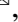
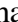


Supervised Fine-tuning *in turn* Improves Visual Foundation Models

Xiaohu Jiang^{1,2}, Yixiao Ge^{2,3}, Yuying Ge³,
Chun Yuan¹, Ying Shan^{2,3},

¹Shenzhen International Graduate School, Tsinghua University

²ARC Lab, Tencent PCG ³Tencent AI Lab

jiangxh21@mails.tsinghua.edu.cn,

{yixiaoge, yuyingge, yingsshan}@tencent.com,


yuanc@sz.tsinghua.edu.cn

Abstract

Image-text training like CLIP has dominated the pre-training of vision foundation models in recent years. Subsequent efforts have been made to introduce region-level visual learning into CLIP’s pretraining but face scalability challenges due to the lack of large-scale region-level datasets. Drawing inspiration from supervised fine-tuning (SFT) in natural language processing such as instruction tuning, we explore the potential of fine-grained SFT in enhancing the generation of vision foundation models after their pretraining. Thus a two-stage method ViSFT is proposed to unleash the fine-grained knowledge of vision foundation models. In ViSFT, the vision foundation model is enhanced by performing visual joint learning on some in-domain tasks and then tested on out-of-domain benchmarks. With updating using ViSFT on 8 V100 GPUs in less than 2 days, a vision transformer with over 4.4B parameters shows improvements across various out-of-domain benchmarks including vision and vision-linguistic scenarios.

1. Introduction

Training of vision foundation models has witnessed significant progress in recent years [5, 12, 22, 31, 51, 57, 66, 67]. Among these developments, the image-text representation learning, exemplified by models such as CLIP [57], has become the mainstream approach for training vision foundation models, achieving state-of-the-art performance across various vision and vision-language tasks. Furthermore, efforts like GLIP [41] and RegionCLIP [82] aim to extend CLIP’s capabilities by learning region-level visual representations during pretraining, thereby facilitating fine-grained

*This work was done when Xiaohu Jiang was interning at ARC Lab, Tencent PCG. Code shall be released at <https://github.com/TencentARC/ViSFT>.  Corresponding author.

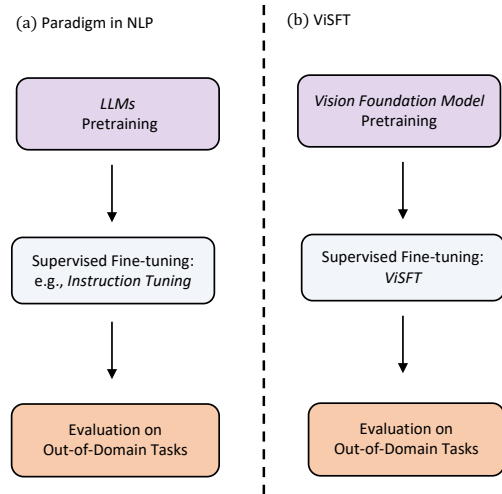


Figure 1. Drawing inspiration from the training paradigm in NLP, we perform ViSFT on vision foundation models after their pre-training and subsequently evaluate them on out-of-domain tasks.

downstream vision tasks. However, these efforts face scalability challenges due to the lack of large-scale region-level datasets.

In the realm of natural language processing, the aforementioned challenge is addressed by employing supervised fine-tuning (SFT) following the pretraining of large language models, such as through instruction tuning [29, 46, 60, 72, 83]. By generating detailed task descriptions as instructions, the model undergoes SFT to understand and follow the instructions. Drawing inspiration from the NLP SFT, we investigate the potential of implementing pure **Vision SFT** (which we term **ViSFT**) to enhance the generalization capabilities of vision foundation models as shown in Figure 1.

Our findings suggest that the representation and generalization of the visual transformer within a CLIP model can

indeed be improved following ViSFT. In essence, ViSFT is able to unleash fine-grained details within the visual transformer that may have been overlooked during image-text pretraining. We speculate that this method assists the vision transformer in identifying a more optimal subspace.

In ViSFT, we incorporate the visual transformer as the backbone network connected to the heads of various in-domain vision tasks for joint learning. We opt for object-level tasks on COCO [42], including detection, segmentation, and captioning. Researchers typically train LoRA [26] for various tasks and then choose the corresponding LoRA weights during inference, meaning that different LoRA weights store their own task-specific knowledge. Similarly, we use LoRA weights to preserve the unleashed information. Another benefit of LoRA tuning is its lightweight nature, which lowers training costs.

ViSFT differs from previous multi-task training approaches [6, 10, 27, 38, 76, 77], which fine-tune on in-domain task training splits and then maximize performance on validation splits. Our goal is to obtain fine-grained information through the joint learning of in-domain tasks (e.g., detection, segmentation), thereby developing a vision transformer backbone with superior representation, and then evaluate the model on out-of-domain benchmarks (e.g., OCR, GOI [40]) as illustrated in Figure 2. Since we do not need to maximize the performance on in-domain tasks, there is no requirement to design intricate task heads for ViSFT, such as multi-task mechanisms for resolving task conflicts [15, 37, 84], making ViSFT more flexible.

Another challenge lies in ensuring that knowledge learned from in-domain tasks can be effectively transferred to the vision transformer backbone, rather than being trapped in task heads. To address this, we divide ViSFT into two stages. In the first stage, we train the corresponding in-domain task heads while keeping the vision transformer backbone frozen. In the second stage, we introduce LoRA parameters to the vision transformer backbone and freeze the task heads, enabling the knowledge to be transferred exclusively to the LoRA parameters.

Our experiments demonstrate that by undergoing ViSFT updating on 8 V100-SXM2-32GB GPUs in less than 2 days, a CLIP vision transformer with a model size exceeding 4.4B exhibits improvements across 6 different benchmarks, including vision and vision-linguistic scenarios (despite not performing SFT on the CLIP’s text encoder). Our contributions can be summarized as follows:

- We showcase the potential of fine-grained supervised fine-tuning (SFT) in enhancing the generalization capabilities of vision foundation models.
- A two-stage ViSFT process is proposed to effectively unleash the fine-grained knowledge of vision foundation models.
- The performance of visual foundation models has shown

improvements across various benchmarks in both visual and vision-linguistic scenarios with lightweight training.

2. Related Work

Pretraining of Vision Foundation Models has experienced considerable progress in recent years. Following the introduction of the Vanilla Vision Transformer (ViT) [12], numerous pretraining paradigms have been explored for vision transformers, including supervised pretraining on large-scale image datasets [11, 65], self-supervised learning strategies [5, 51], masked image modeling techniques [22, 53], and more. Notably, image-text pretraining methods [31, 57, 78] such as CLIP have emerged as the predominant approach for training foundational vision models. This method leverages extensive image-text data to pretrain models, aiming to learn the correspondence between images and text.

Moreover, efforts like GLIP [41] and RegionCLIP [82] intend to introduce region-level visual representation learning into CLIP’s pretraining process, thereby enhancing the performance of fine-grained downstream vision tasks. However, these endeavors encounter challenges in scaling up the model size due to the scarcity of large-scale region-level detection and grounding data. As a result, CLIP remains the prevailing paradigm in visual representation learning, supported by extensive image-text datasets.

Recent EVA-CLIP series [13, 14, 66] achieve state-of-the-art performance on several zero-shot benchmarks. EVA first performs masked image modeling on scratch-based vision transformers to reconstruct the features of a CLIP’s vision encoder. Then, the vision encoder of CLIP is replaced with the trained vision transformers for image-text pretraining. EVA successfully scales the vision transformer to over 4.4 billion parameters. While BLIP-2 [39] employs a bridge model (q-former) to integrate EVA-CLIP-G with large language models (LLMs), achieving state-of-the-art performance on various visual-language benchmarks. Our ViSFT has explored the potential of fine-grained supervised fine-tuning in enhancing the generalization capabilities of both EVA-CLIP and BLIP-2.

Visual-Linguistic Instruction Tuning represents a simple yet effective supervised fine-tuning (SFT) strategy for enhancing the generalizability of foundational models. Notably, natural language processing (NLP) instruction tuning [29, 46, 60, 72, 83] has achieved promising results in zero-shot learning by utilizing a small number of examples and a set of natural language instructions to guide the model in learning new tasks. There are generally two methods for constructing instruction datasets: data integration from annotated natural language datasets [46, 60] and generating outputs using LLMs [71, 75]. Based on the collected IT dataset, a pre-trained model can be directly fine-tuned

in a fully-supervised manner. Among these techniques, HINT [29] adopts a hypernetwork to convert instructions into adapter and prefix parameters, which is akin to how ViSFT stores fine-grained information in LoRA parameters.

Besides text-only domains, instruction tuning has been applied in multimodal domains [3, 17, 43, 74, 81]. MULTIINSTRUCT [74] is a multimodal instruction tuning dataset comprising 62 diverse tasks in a unified seq-to-seq format. LLaVA (13B) [43] is a large multimodal model developed by connecting the visual encoder of CLIP (400M) [57] with the language decoder LLaMA (7B) [68]. GPT-4 is employed to convert image-text pairs into an appropriate instruction-following format for LLaVA’s dataset. While the above studies have achieved success in text-only and multimodal domains, the vision-only domain SFT has not yet been extensively explored.

Multi-Task Training employs foundation models as the backbone, coupled with multiple task-specific heads. Typically, multi-task training involves fine-tuning the backbone and task-specific heads concurrently on downstream tasks’ training splits and maximizing performance on validation splits, which are in-domain.

There has been extensive development in multi-task training across vision [21, 63, 64, 79, 80], language [20, 44, 45, 59, 61], and multimodal domains [32, 35, 56]. Recent efforts aim to perform multi-task training using a single, generic model [32, 38, 76, 77, 84]. However, such attempts often face challenges due to task and domain conflicts, leading to the development of domain alignment methods and mechanisms to mitigate task conflicts.

ViSFT departs from traditional multi-task training approaches by obtaining fine-grained information through joint learning of in-domain tasks while evaluating performance on out-of-domain tasks. Additionally, rather than tuning LoRA and task heads simultaneously, ViSFT is divided into two stages. Since there is no need to maximize performance on in-domain tasks, ViSFT does not require domain alignment methods or task conflict alleviation mechanisms, making it more flexible and easier to implement.

3. Method

3.1. Tasks and Datasets

To ensure that ViSFT remains both simple and fine-grained while eliminating the need to create new datasets, we opted to train our model using the COCO [42] dataset. This dataset provides a diverse range of annotations for each image, including bounding boxes, instance-specific segmentation masks, natural language descriptions, and panoptic segmentation masks (a combination of instance and semantic segmentation). Additionally, 250k-person instances are annotated with keypoints. As depicted in Table 1, these an-

Tasks	Annotations	Heads
Object Detection	bounding boxes with 80 object categories	Detr
Instance Segmentation	per-instance segmentation masks	Mask2former
Image Captioning	natural language descriptions of the images	LSTM
Panoptic Segmentation	full scene segmentation with thing and stuff	Mask2former
Pose Estimation	person instances labeled with keypoints	VitPose

Table 1. An overview of task categories and annotations in COCO, along with their associated task heads for implementation. Annotations excluded from our proposed solution are denoted in Gray.

Model	Layers	Hidden size	Patch size	MLP size	Heads	Params
EVA-ViT-G [66]	40	1408	14	6144	16	1B
EVA-ViT-E [66]	64	1792	14	15360	16	4.4B

Table 2. Details of EVA-ViT model variants employed in our experiments: EVA-ViT-G and EVA-ViT-E, both with over 1 Billion parameters, are derived from EVA-CLIP-G and EVA-CLIP-E models, respectively.

notations enable fine-grained learning for every image.

Following the ablation studies in Sec 4.4, we ultimately selected object detection, instance segmentation, and image captioning as the in-domain tasks. Moreover, tasks on COCO offer a variety of off-the-shelf task heads, obviating the need to develop new task heads.

3.2. Model Details

In this section, we outline the process of conducting ViSFT on the vision foundation model as illustrated in Figure 2. The entire model training procedure is divided into two stages. During the first stage, we employ the pre-trained vision transformer from an EVA-CLIP model to serve as the backbone network and freeze it. Detection, segmentation, and caption heads are then independently connected for fine-tuning. This step aims to obtain task heads that are compatible with the vision transformer features. In the second stage, the vision transformer is augmented with LoRA weights, and all task heads are connected for fine-tuning. Aside from the added LoRA weights, other modules will remain frozen. This approach ensures that fine-grained information obtained through joint learning is directed towards the LoRA parameters.

EVA Vision Transformer. We select the vision transformer from EVA-CLIP [66] as the vision foundation model, given its state-of-the-art performance and the architecture that is basically consistent with the vanilla ViT [12]. As demonstrated in Table 2, we conducted experiments using two model sizes: EVA-ViT-G and EVA-ViT-E.

LoRA Update Matrices. For a pre-trained weight matrix $W_{q/v} \in \mathbb{R}^{d \times k}$ within the query and value embedding layers of EVA-ViT, we impose a constraint on their updates by introducing a low-rank decomposition: $W_{q/v} + \Delta W = W_{q/v} + BA$, where $B \in \mathbb{R}^{d \times r}$ and $A \in \mathbb{R}^{r \times k}$, and rank

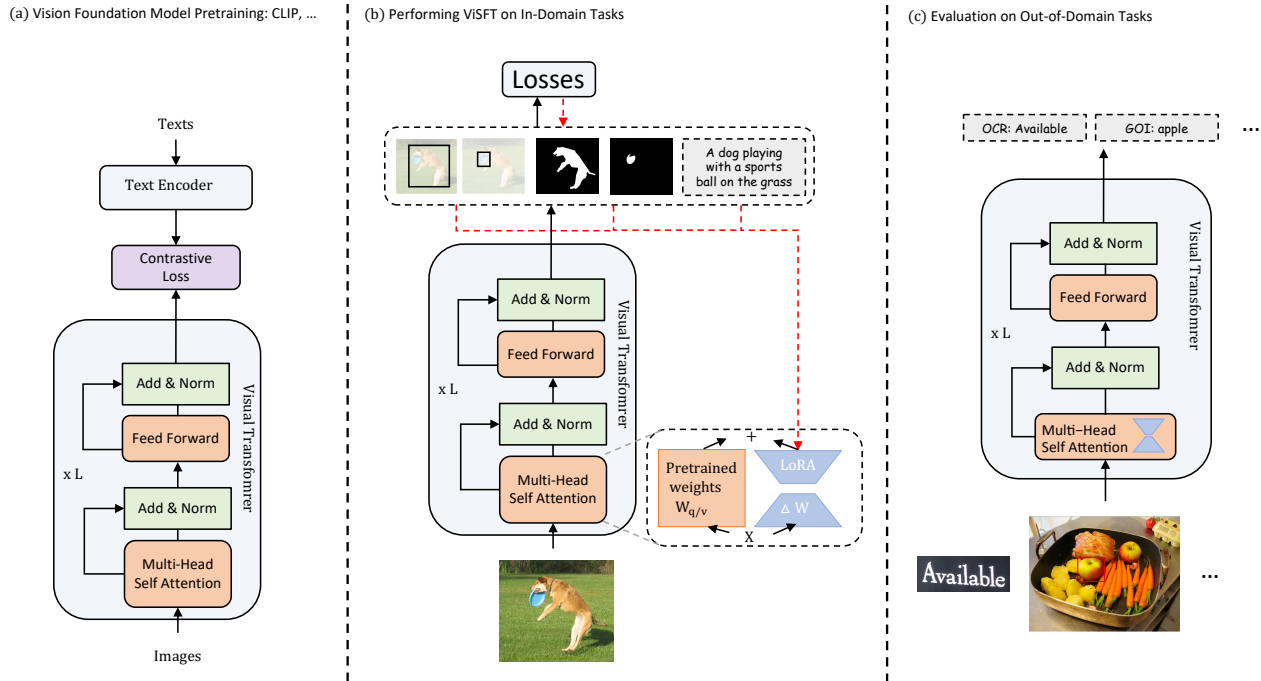


Figure 2. An overview of our proposed method is as follows: (a) First, a vision foundation model is pretrained such as CLIP-ViT. (b) Next, we execute ViSFT to update the LoRA weights and retain the fine-grained information through joint learning of in-domain tasks. (c) Finally, in conjunction with the updated LoRA weights, evaluations on multiple out-of-domain tasks exhibit considerable enhancement. ‘‘OCR’’ refers to the optical character recognition task, while ‘‘GOI’’ denotes the grounded object identification task.

$r < \min(d, k)$. During the second stage of training, the weight matrices W_q and W_v are frozen, preventing them from receiving gradient updates, while A and B contain trainable parameters. For $h_{q/v} = W_{q/v}x$, the forward pass yields:

$$h_{q/v} = W_{q/v}x + \Delta Wx = W_{q/v}x + BAx \quad (1)$$

Detection Head. Among the available detection heads, Detr [4] is the first to incorporate transformers, which simplifies the detection head design, eliminates the need for intricate post-processing techniques such as non-maximum suppression, and supports single-scale feature input from vision transformers. While Detr exhibits slow convergence, it is important to note that we don’t pursue superior performance on these in-domain task heads. Instead, we employ these task heads as a bridge to restore fine-grained information of the vision transformer.

Detr generates a fixed number of learnable query embeddings, which serve as input to the image decoder. These queries interact with one another via self-attention and interact with flattened image features through cross-attention layers. Subsequently, MLP and linear heads are employed for bounding box and label prediction, respectively. Finally, a bi-partite matching mechanism is used to assign predic-

tions to ground truth boxes.

Segmentation Head. We utilize Mask2former [9] as the segmentation head. As a unified framework for segmentation tasks, Mask2former is capable of handling both instance segmentation and panoptic segmentation tasks, thereby providing convenience for experimenting with various segmentation annotations. To facilitate the use of vision transformers as the backbone, we have modified the input feature levels of Mask2former to 1.

Mask2former also generates a fixed number of query embeddings. The segmentation mask representations are derived from the dot product between the decoder’s final-layer hidden state of the j -th embedding and a per-pixel feature map:

$$q_i^{\text{mask}} = \text{Upsample}\left(\text{MLP}(q_i) \odot \mathcal{R}(\mathcal{G}(\mathcal{F}_0) + \mathcal{H}(\mathcal{F}_1^{\text{enc}}))\right), \quad (2)$$

where \mathcal{G} is a 1×1 convolution layer followed by a Group Normalization (GN), \mathcal{H} is a 1×1 convolution followed by a GN and a bilinear upsampling, and \mathcal{R} is a 3×3 convolution followed by a GN, a ReLU, and a 1×1 convolution. \mathcal{F}_0 and $\mathcal{F}_1^{\text{enc}}$ represent the per-pixel feature maps produced by the backbone and encoder, respectively.

Captioning Head. Following [73], we employ a classic

Long Short-Term Memory (LSTM) network that generates a caption by producing one word at each time step, conditioned on a context vector, the previous hidden state, and the previously generated words.

$$\begin{pmatrix} i_t \\ f_t \\ o_t \\ g_t \end{pmatrix} = \begin{pmatrix} \sigma \\ \sigma \\ \sigma \\ \tanh \end{pmatrix} T_{D+m+n,n} \begin{pmatrix} E_{y_{t-1}} \\ h_{t-1} \\ \hat{z}_t \end{pmatrix} \quad (3)$$

$$\begin{aligned} c_t &= f_t \odot c_{t-1} + i_t \odot g_t \\ h_t &= o_t \odot \tanh(c_t) \end{aligned} \quad (4)$$

Here, i_t , f_t , o_t , g_t , and h_t represent the input, forget, memory, output, and hidden states of the LSTM, respectively. The context vector denoted as $\hat{z} \in \mathbb{R}^D$, captures the visual information associated with a specific input location. The embedding matrix $E \in \mathbb{R}^{m \times K}$ is also considered. Let m and n represent the embedding and LSTM dimensionality, respectively, while σ and \odot denote the logistic sigmoid activation and element-wise multiplication, respectively.

Trainable Parameters. The trained parameters comprise two parts: in the first stage, the parameters of each task head are trained, while in the second stage, the weights of LoRA are trained. In terms of parameter size settings, taking EVA-ViT-E as an example, the total parameter size of all task heads amounts to 36.8M. We set the size of the two parts to be roughly equal, thus setting the rank of LoRA to 64, resulting in a parameter size of 29.4M. Subsequent ablation experiments in sec 4.4 demonstrate that the size of LoRA parameters has minimal impact on the results.

4. Experiments

4.1. Evaluation Benchmarks

We focus on performance on out-of-domain tasks and datasets that are not included as part of the supervised vision finetuning, encompassing both visual and visual-linguistic benchmarks:

(1) Optical Character Recognition (OCR): After freezing the vision transformer and its corresponding LoRA weights, we follow the approach in [2] to train a lightweight head for optical character recognition. Utilizing the frozen backbone weights, we employ the MJSynth [30] and SynthText [19] datasets for training and evaluate the performance on a combined set of multiple OCR datasets, including IC03 [48], IC13 [33], IC15 [34], SVTP [54], SVT [70], and IIIT [50].

(2) Grounded Object Identification: We evaluate the model’s performance on the M³IT dataset [40], which involves classifying an object specified in an image.

(3) Image Classification: We replace EVA-CLIP’s visual encoder with the fine-tuned EVA-ViT and perform zero-shot classification on ImageNet-1K [11] and its

variants (ImageNet-A [25], ImageNet-R [24], ImageNet-Sketch [69]), as well as other classification datasets [16, 23, 36, 62].

(4) Image-Text Retrieval: We examine the zero-shot retrieval performance on COCO [8] and Flickr30K [55] for both EVA-CLIP-E and BLIP-2, in which the vision encoder is replaced by EVA-ViT-E and EVA-ViT-G, respectively.

(5) Visual Question Answering: After fine-tuning the visual encoder of BLIP-2, we conduct a quantitative evaluation of the zero-shot visual question answering task on VQAv2 [18], GQA [28], and OK-VQA [49].

(6) Captioning: Captioning performance on the unseen NoCaps dataset [1] is also evaluated.

4.2. Implementation Details

During the first stage of training, Detr [4] serves as the detection head, featuring six encoder layers and six decoder layers. The encoder dimension is 128, the decoder dimension is 256, and the MLP dimension is 1024. For the segmentation head, Mask2former [9] consists of six encoder layers and nine decoder layers. The encoder dimension is 256, the encoder MLP dimension is 512, the decoder dimension is 256, and the decoder MLP dimension is 1024. Both Detr and Mask2former share the following settings: the number of attention heads is 8, the number of input query embeddings is 100, the batch size is 1 per GPU, the number of feature levels is 1, and the learning rate is $5e-5$. Both models are trained for 150k iterations.

With respect to the captioning head, we primarily adhere to the settings presented in [73]. The LSTM encoder and decoder dimensions are both 384, the batch size is 32 per GPU, the learning rate is $4e-4$, and the training proceeds for 100k iterations. All task head training utilizes the AdamW optimizer [47], embraces a cosine learning rate strategy, and incorporates a warmup of 2k iterations. The training for each task head is executed using 8 Nvidia Volta V100-SXM2-32GB GPUs. The training of various task heads can be conducted concurrently, with the first stage of training requiring less than 3 days to finish.

During the second stage of training, we jointly train EVA-ViT on multiple tasks. At each iteration, we randomly select a task to fill a batch of samples. We simply assign a comparable sampling probability for each task (0.4 for captioning, 0.3 for both detection and segmentation). In our implementation, we employ 8 NVIDIA Volta V100-SXM2-32GB GPUs (batch size 1 per GPU for detection and segmentation, batch size 8 per GPU for captioning) in a distributed manner, using PyTorch [52]. To alleviate the CUDA memory pressure, we have enabled optimizer state sharding. It uses the ZeRO optimizer state sharding method as described in [58]. Additionally, gradient checkpointing [7] is activated. The AdamW optimizer is utilized with a learning rate of $1e-5$ and a warm-up cosine learning rate

Model	Params	Iters	Accuracy
EVA-ViT-G	1.0B	0k	44.4
EVA-ViT-G _{ViSFT}	1.0B	5k	46.9(+2.5)
EVA-ViT-G _{ViSFT}	1.0B	15k	47.6(+3.2)

Table 3. Evaluation of optical character recognition performance before and after Vision SFT implementation. “Accuracy” represents the ratio of correct word instances to the total number of word instances (%). “Iters” refers to the number of iterations updated during the second stage.

schedule (using 2000 warm-up iterations).

The training process continues for 50k iterations, with checkpoints saved every 5k iterations. The second stage of training requires less than 2 days to complete. We denote the model after 5k iterations as the default ViSFT setting, as it shows improvement on the majority of benchmarks.

4.3. Main Results

Optical Character Recognition (OCR). Optical Character Recognition (OCR) aims to extract textual information from images, posing a fine-grained and challenging task due to the variability in fonts, colors, sizes, and orientations of the text within images. Consequently, OCR serves as an effective benchmark to evaluate the capability of a visual foundation model in capturing the fine-grained and semantic information of an image.

In line with the methodology proposed in [2], we implement a vision transformer as the backbone of our model, freezing both the backbone and its corresponding LoRA weights. Following this, we train a 4-layer lightweight transformer head specifically designed for the OCR task. To evaluate the effectiveness of our approach, we perform experiments on a diverse collection of OCR datasets [33, 34, 48, 50, 54, 70] and report the average accuracy. The results presented in Table 3 demonstrate that after applying the ViSFT, the performance of optical character recognition can be improved by at least 2.5 points, which indicates that the vision transformer effectively regains fine-grained information and is able to capture both the intricate details and semantic information of the image.

Grounded Object Identification. Grounded Object Identification (GOI) involves classifying a specified object in an image using the [CLS] token feature of vision transformers. This fine-grained task was not seen during EVA-CLIP’s pretraining or our ViSFT. After probing the classification head for 30 epochs on the M³IT dataset, both EVA-ViT-G and EVA-ViT-E exhibit an enhancement ranging from 0.3 to 0.6 points, as depicted in Table 4. The improvement is more pronounced for EVA-ViT-G, which is a smaller model. These results indicate that ViSFT can bolster the model’s generalization performance, with more significant improvements observed in smaller models, which possess

Model	Params	Iters	M ³ IT [40] val	
			Top-1 Acc	Top-5 Acc
EVA-ViT-G	1.0B	0k	52.3	87.3
EVA-ViT-G _{ViSFT}	1.0B	5k	52.9(+0.6)	87.5(+0.2)
EVA-ViT-G _{ViSFT}	1.0B	15k	52.9(+0.6)	87.7(+0.4)
EVA-ViT-E	4.4B	0k	54.9	88.3
EVA-ViT-E _{ViSFT}	4.4B	5k	55.2(+0.3)	88.7(+0.4)

Table 4. Performance of grounded object identification under various conditions. We report the Top-1 and Top-5 accuracies (%) on M³IT’s validation set with improvements denoted in brackets, e.g., (+0.6). “Iters” refers to the number of iterations updated during the second stage.

	ImageNet-A [25]	ImageNet-R [24]	ImageNet-S [69]	ImageNet-1K [11]	EuroSAT [23]	CIFAR-10 [36]	CIFAR-100 [36]	GTSRB [62]	Caltech-101 [16]
EVA-CLIP-E [66]	82.1	94.5	71.6	82.0	65.8	99.3	93.1	67.7	90.5
EVA-CLIP-E _{ViSFT}	82.4	94.6	71.7	82.1	67.1	99.4	93.2	67.8	90.6

Table 5. Zero-shot image classification results on ImageNet-1K and its variants, as well as additional classification datasets. Top-1 accuracy (%) on validation sets is reported. Results exhibiting notable improvements are emphasized in **Bold**. The number of iterations updated during the second stage in this case is 5k.

fewer parameters and are more prone to losing fine-grained information during image-text pretraining.

Image Classification. In Table 5, we further exhibit the effectiveness and robustness of our approach across 9 zero-shot image classification benchmarks. We conduct zero-shot classification on EVA-CLIP-E before and after visually supervised fine-tuning, observing improvements across all 9 datasets. Notable enhancements are evident on datasets consisting of adversarial and unmodified examples, such as ImageNet-A [25] (increasing from 82.1% to 82.4%) and EuroSAT [23] (rising from 65.8% to 67.1%), indicating that fine-grained information can strengthen the model’s robustness to real-world perturbations.

Image-Text Retrieval. Table 6 presents the zero-shot image and text retrieval results on Flickr30K and COCO. Upon implementing ViSFT, EVA-CLIP-E exhibits enhancements in both text and image retrieval, with a more significant impact observed in image retrieval tasks. Notably, it shows a 1.1% increase in image retrieval performance, as assessed by COCO’s Recall@5 metric. This is attributable to the model’s ability to better understand and extract relevant features from images when paired with corresponding texts.

We further conducted evaluations on paradigms beyond EVA-CLIP, such as BLIP-2. Owing to the constraints in resources, we did not retrain a q-former. Instead, we lever-

Model	Iters	Text Retrieval		Image Retrieval	
		Flickr30k R@5	COCO R@5	Flickr30k R@5	COCO R@5
EVA-CLIP-E [66]	0k	99.4	87.6	94.3	74.9
EVA-CLIP-E _{ViSFT}	5k	99.4	87.7(+0.1)	94.3	75.2(+0.3)
EVA-CLIP-E _{ViSFT}	50k	99.5(+0.1)	87.6	94.8(+0.5)	76.0(+1.1)
BLIP-2 ViT-G [66]	0k	99.9	94.2	96.8	84.0
BLIP-2 ViT-G _{ViSFT}	5k	99.9	94.3(+0.1)	96.9(+0.1)	84.1(+0.1)

Table 6. Comparison of image-text retrieval performance across various settings. Results are assessed using Recall@5 (%). Performance for both Flickr30K and COCO datasets are reported, with evaluations conducted on EVA-CLIP and BLIP-2. Notable improvements are highlighted in **Bold**. Owing to the constraints in resources, we did not retrain a q-former of BLIP-2. “Iters” refers to the number of iterations updated during the second stage.

Model	Params	Iters	VQAv2	OK-VQA	GQA
BLIP-2 ViT-G OPT ^s [39]	3.8B	0k	51.9	31.5	32.6
BLIP-2 ViT-G OPT ^s _{ViSFT}	3.8B	5k	52.0	31.5	32.6
BLIP-2 ViT-G OPT ^s _{ViSFT}	3.8B	20k	52.0	31.7	32.7
BLIP-2 ViT-G OPT ^l [39]	7.8B	0k	55.1	35.4	35.3
BLIP-2 ViT-G OPT ^l _{ViSFT}	7.8B	5k	55.2	35.5	35.3
BLIP-2 ViT-G OPT ^l _{ViSFT}	7.8B	20k	55.3	35.7	35.5

Table 7. Zero-shot visual question answering results. Metrics include accuracy for VQAv2, OK-VQA, and GQA (%). Evaluations are conducted on BLIP-2 ViT-G OPT_{2.7B} (designated as OPT^s) and BLIP-2 ViT-G OPT_{6.7B} (designated as OPT^l). Due to limited resources, we did not retrain a q-former of BLIP-2.

aged the pre-trained weights of BLIP-2 from its first stage to perform a zero-shot evaluation. As illustrated in Table 6, after implementing fine-grained tuning on BLIP-2’s visual encoder, we observed phenomena similar to those of EVA-CLIP, which further substantiates our conclusions.

Visual Question Answering. We assessed the zero-shot visual question answering performance of BLIP-2 ViT-G OPT_{2.7B} and BLIP-2 ViT-G OPT_{6.7B} using benchmarks such as VQAv2 [18], GQA [28], and OK-VQA [49]. As depicted in Table 7, the models performing ViSFT on their visual encoder either maintain or enhance their performance across all three benchmarks. The improvement is a bit more pronounced on OK-VQA, suggesting that ViSFT provides benefits for out-of-domain datasets. Moreover, the performance improvement is slightly more evident when scaling the language model from 2.7B to the larger 6.7B version, indicating that our ViSFT can preserve the visual-linguistic alignment when the language model is scaled up even without retraining the q-former.

Image Captioning. We evaluated the image captioning performance of our Vision SFT in conjunction with BLIP-2 ViT-G OPT on the NoCaps dataset, which was not used during the training phase. Our findings indicate that ViSFT

Model	Params	Iters	CIDEr
BLIP-2 ViT-G OPT ^s [39]	3.8B	0k	100.9
BLIP-2 ViT-G OPT ^s _{ViSFT}	3.8B	5k	101.3(+0.4)
BLIP-2 ViT-G OPT ^s _{ViSFT}	3.8B	15k	102.1(+1.1)

Table 8. NoCaps caption performance. Results are reported using the CIDEr metric, which measures the similarity between generated captions and ground-truth captions (higher values are better). Experiments are conducted on BLIP-2 ViT-G OPT_{2.7B} (designated as OPT^s). Q-former of BLIP-2 is not retrained due to limited resources. “Iters” refers to the number of iterations updated during the second stage.

Rank	COCO	
	Text Retrieval R@5	Image Retrieval R@5
$r = 8$	87.7	75.1
$r = 16$	87.7	75.1
$r = 32$	87.8	75.0
$r = 64$	87.7	75.2

Table 9. Ablation analysis of LoRA with varying ranks. Results are presented for text retrieval (R@5), and image retrieval (R@5).

is able to enhance captioning performance on the unseen dataset. Results are provided in Table 8.

4.4. Ablation Studies

In the subsequent sections, we examine the critical designs of our ViSFT in conjunction with EVA-CLIP-E. Unless explicitly stated, image-text retrieval performance on the COCO dataset is evaluated.

Effects of LoRA Rank. In the rank configuration for LoRA, as mentioned before, we employed the default value of $r = 64$, which results in comparable parameter sizes for LoRA and task heads within our experimental setup. Table 9 demonstrates that LoRA exhibits competitive performance across various rank settings. Consequently, we maintain the original default configuration, and the additional costs incurred compared to smaller rank settings are negligible.

Training Data Size. Table 10 indicates that utilizing the full training dataset yields slightly more competitive performance, suggesting that there may be room for improvement if we can leverage more data annotated similarly to COCO. We defer this exploration to future work, as the impact of training data size is marginal, for instance, increasing the training data size from 25% to 100% only enhances the performance by 0.1% in the image-text retrieval task.

Training Strategies. In the second stage, there are three potential strategies for performing vision fine-tuning. The classic approach involves fine-tuning both the task heads and the backbone simultaneously. However, as Table 11

Data Size	COCO	
	Text Retrieval R@5	Image Retrieval R@5
25%	87.6	75.1
50%	87.6	75.1
100%	87.7	75.2

Table 10. Ablation of training data size on image-text retrieval tasks: K% indicates the use of K% of the available training data.

Head LR	COCO	
	Text Retrieval R@5	Image Retrieval R@5
ViT LR×0	87.7	75.2
ViT LR×0.1	87.6	75.1
ViT LR×1	87.6	75.0

Table 11. Ablation analysis of employing various task head learning rates in the second training stage: "ViT LR ×0" indicates freezing the task heads, "ViT LR ×1" denotes simultaneous fine-tuning of LoRA weights and task heads, and "ViT LR ×0.1" represents fine-tuning task heads with a learning rate that is 0.1 times smaller than the learning rate applied to ViT's LoRA weights.

Setting	ImageNet-1K	COCO	
	Classification Top-1	Text Retrieval R@5	Image Retrieval R@5
Default	82.1	87.7	75.2
w/ pose	82.1	87.7	75.1 ↓
r/ panoptic	82.1	87.8 ↑	75.1 ↓
w/o detection	82.0 ↓	87.9 ↑	75.2
w/o segmentation	82.0 ↓	87.8 ↑	75.1 ↓
w/o caption	82.0 ↓	87.8 ↑	75.2

Table 12. Ablation analysis of task type selection. Evaluation focuses on zero-shot image classification and image-text Retrieval. Default setting incorporates object detection, instance segmentation and image captioning. "w/" denotes "with", "w/o" signifies "without" and "r/panoptic" represents "instance segmentation is replaced by panoptic segmentation". Arrows are used to represent the increase or decrease relative to the default setting.

demonstrates, this method yields suboptimal performance. As previously mentioned, fine-grained information learned from different annotations can be trapped within the task heads. Consequently, an alternative solution is to minimize the learning rate of the task heads, for example, setting it to 1/10 of the backbone's learning rate. Nonetheless, as observed in Table 11, the performance remains unsatisfactory, suggesting that fine-grained information is indeed prone to be trapped in the task heads. Therefore, we propose freezing the task heads, and the results indicate that this strategy performs better.

Selection of Task Types. In our default configuration, we adopt object detection, image captioning, and instance



Figure 3. Visualization of [CLS] token's attention distribution. Experiments are conducted on the last layer of EVA-ViT-G. Attended image patches are highlighted.

segmentation on COCO. To analyze the effects of various tasks, we conduct experiments by either adding new tasks, such as pose estimation, replacing instance segmentation with panoptic segmentation, or independently removing each task from the joint-training tasks. For pose estimation, we employ the ViTPose task head, which utilizes a vision transformer as the backbone and requires only a single-scale input feature. For panoptic segmentation, which combines instance segmentation and semantic segmentation, we maintain the use of the mask2former head to ensure a fair comparison.

Table 12 demonstrates that adding a new task, such as pose estimation, does not yield further performance improvements. This is reasonable, as not all images in COCO contain person instances that would benefit from pose keypoint annotations. A similar phenomenon can be observed in instruction tuning [72]: not all task clusters benefit the foundation model, and minimal impact is observed from the sentiment analysis cluster.

The results for instance segmentation and panoptic segmentation are competitive, as semantic annotations are more coarse-grained than instance annotations. This indicates that instance annotations possess sufficient granularity for effectively performing our ViSFT.

Upon removing any of the three tasks, the zero-shot image classification performance deteriorates, despite exhibiting competitive results in text retrieval. This aligns with observations from instruction tuning [72], emphasizing the importance of task diversity for executing supervised fine-tuning. When the number of fine-tuning tasks is limited, the model's generative capabilities are also constrained.

4.5. Visualization

To further substantiate the efficacy of our approach, we have conducted a visualization of ViSFT. The image patches of EVA-ViT-G are reshaped into a 2D configuration following the insertion of the [CLS] token, and we visualize the attention distribution of the [CLS] token across these patches. As depicted in Figure 3, after applying ViSFT, the [CLS] token not only attends to nearby patches (highlighted at the top of the images) but also focuses on more distant objects.

This suggests that ViSFT assists vision foundation models in capturing fine-grained information from image patches.

5. Conclusion

Drawing inspiration from natural language processing, we explore the potential of fine-grained supervised fine-tuning (SFT) to enhance the generalization and representation capabilities of vision foundation models after pretraining. We propose a two-stage method, termed "ViSFT," to effectively unleash the fine-grained knowledge embedded within these models. Through our lightweight training process, the performance of vision foundation models exhibits improvements across a wide range of out-of-domain benchmarks in both visual and vision-linguistic scenarios.

References

- [1] Harsh Agrawal, Karan Desai, Yufei Wang, Xinlei Chen, Rishabh Jain, Mark Johnson, Dhruv Batra, Devi Parikh, Stefan Lee, and Peter Anderson. Nocaps: Novel object captioning at scale. In *Proceedings of the IEEE/CVF international conference on computer vision*, pages 8948–8957, 2019. 5
- [2] Rowel Atienza. Vision transformer for fast and efficient scene text recognition. In *International Conference on Document Analysis and Recognition*, pages 319–334. Springer, 2021. 5, 6
- [3] Tim Brooks, Aleksander Holynski, and Alexei A Efros. Instructpix2pix: Learning to follow image editing instructions. In *Proceedings of the IEEE/CVF Conference on Computer Vision and Pattern Recognition*, pages 18392–18402, 2023. 3
- [4] Nicolas Carion, Francisco Massa, Gabriel Synnaeve, Nicolas Usunier, Alexander Kirillov, and Sergey Zagoruyko. End-to-end object detection with transformers. In *European conference on computer vision*, pages 213–229. Springer, 2020. 4, 5
- [5] Mathilde Caron, Hugo Touvron, Ishan Misra, Hervé Jégou, Julien Mairal, Piotr Bojanowski, and Armand Joulin. Emerging properties in self-supervised vision transformers. In *Proceedings of the IEEE/CVF international conference on computer vision*, pages 9650–9660, 2021. 1, 2
- [6] Rich Caruana. Multitask learning. *Machine learning*, 28: 41–75, 1997. 2
- [7] Tianqi Chen, Bing Xu, Chiyuan Zhang, and Carlos Guestrin. Training deep nets with sublinear memory cost. *arXiv preprint arXiv:1604.06174*, 2016. 5
- [8] Xinlei Chen, Hao Fang, Tsung-Yi Lin, Ramakrishna Vedantam, Saurabh Gupta, Piotr Dollár, and C Lawrence Zitnick. Microsoft coco captions: Data collection and evaluation server. *arXiv preprint arXiv:1504.00325*, 2015. 5
- [9] Bowen Cheng, Ishan Misra, Alexander G Schwing, Alexander Kirillov, and Rohit Girdhar. Masked-attention mask transformer for universal image segmentation. In *Proceedings of the IEEE/CVF conference on computer vision and pattern recognition*, pages 1290–1299, 2022. 4, 5
- [10] Michael Crawshaw. Multi-task learning with deep neural networks: A survey. *arXiv preprint arXiv:2009.09796*, 2020. 2
- [11] Jia Deng, Wei Dong, Richard Socher, Li-Jia Li, Kai Li, and Li Fei-Fei. Imagenet: A large-scale hierarchical image database. In *2009 IEEE conference on computer vision and pattern recognition*, pages 248–255. Ieee, 2009. 2, 5, 6, 1
- [12] Alexey Dosovitskiy, Lucas Beyer, Alexander Kolesnikov, Dirk Weissenborn, Xiaohua Zhai, Thomas Unterthiner, Mostafa Dehghani, Matthias Minderer, Georg Heigold, Sylvain Gelly, et al. An image is worth 16x16 words: Transformers for image recognition at scale. *arXiv preprint arXiv:2010.11929*, 2020. 1, 2, 3
- [13] Yuxin Fang, Quan Sun, Xinggang Wang, Tiejun Huang, Xinlong Wang, and Yue Cao. Eva-02: A visual representation for neon genesis. *arXiv preprint arXiv:2303.11331*, 2023. 2
- [14] Yuxin Fang, Wen Wang, Binhui Xie, Quan Sun, Ledell Wu, Xinggang Wang, Tiejun Huang, Xinlong Wang, and Yue Cao. Eva: Exploring the limits of masked visual representation learning at scale. In *Proceedings of the IEEE/CVF Conference on Computer Vision and Pattern Recognition*, pages 19358–19369, 2023. 2
- [15] William Fedus, Barret Zoph, and Noam Shazeer. Switch transformers: Scaling to trillion parameter models with simple and efficient sparsity. *The Journal of Machine Learning Research*, 23(1):5232–5270, 2022. 2
- [16] Li Fei-Fei, Rob Fergus, and Pietro Perona. Learning generative visual models from few training examples: An incremental bayesian approach tested on 101 object categories. In *2004 conference on computer vision and pattern recognition workshop*, pages 178–178. IEEE, 2004. 5, 6, 1
- [17] Tao Gong, Chengqi Lyu, Shilong Zhang, Yudong Wang, Miao Zheng, Qian Zhao, Kuikun Liu, Wenwei Zhang, Ping Luo, and Kai Chen. Multimodal-gpt: A vision and language model for dialogue with humans. *arXiv preprint arXiv:2305.04790*, 2023. 3
- [18] Yash Goyal, Tejas Khot, Douglas Summers-Stay, Dhruv Batra, and Devi Parikh. Making the v in vqa matter: Elevating the role of image understanding in visual question answering. In *Proceedings of the IEEE conference on computer vision and pattern recognition*, pages 6904–6913, 2017. 5, 7, 1
- [19] Ankush Gupta, Andrea Vedaldi, and Andrew Zisserman. Synthetic data for text localisation in natural images. In *Proceedings of the IEEE conference on computer vision and pattern recognition*, pages 2315–2324, 2016. 5, 1
- [20] Kazuma Hashimoto, Caiming Xiong, Yoshimasa Tsuruoka, and Richard Socher. A joint many-task model: Growing a neural network for multiple nlp tasks. *arXiv preprint arXiv:1611.01587*, 2016. 3
- [21] Kaiming He, Georgia Gkioxari, Piotr Dollár, and Ross Girshick. Mask r-cnn. In *Proceedings of the IEEE international conference on computer vision*, pages 2961–2969, 2017. 3
- [22] Kaiming He, Xinlei Chen, Saining Xie, Yanghao Li, Piotr Dollár, and Ross Girshick. Masked autoencoders are scalable vision learners. In *Proceedings of the IEEE/CVF conference on computer vision and pattern recognition*, pages 16000–16009, 2022. 1, 2

- [23] Patrick Helber, Benjamin Bischke, Andreas Dengel, and Damian Borth. Eurosat: A novel dataset and deep learning benchmark for land use and land cover classification. *IEEE Journal of Selected Topics in Applied Earth Observations and Remote Sensing*, 12(7):2217–2226, 2019. 5, 6, 1
- [24] Dan Hendrycks, Steven Basart, Norman Mu, Saurav Kadavath, Frank Wang, Evan Dorundo, Rahul Desai, Tyler Zhu, Samyak Parajuli, Mike Guo, et al. The many faces of robustness: A critical analysis of out-of-distribution generalization. In *Proceedings of the IEEE/CVF International Conference on Computer Vision*, pages 8340–8349, 2021. 5, 6, 1
- [25] Dan Hendrycks, Kevin Zhao, Steven Basart, Jacob Steinhardt, and Dawn Song. Natural adversarial examples. In *Proceedings of the IEEE/CVF Conference on Computer Vision and Pattern Recognition*, pages 15262–15271, 2021. 5, 6, 1
- [26] Edward J Hu, Yelong Shen, Phillip Wallis, Zeyuan Allen-Zhu, Yuanzhi Li, Shean Wang, Lu Wang, and Weizhu Chen. Lora: Low-rank adaptation of large language models. *arXiv preprint arXiv:2106.09685*, 2021. 2
- [27] Ronghang Hu and Amanpreet Singh. Unit: Multimodal multitask learning with a unified transformer. In *Proceedings of the IEEE/CVF International Conference on Computer Vision*, pages 1439–1449, 2021. 2
- [28] Drew A Hudson and Christopher D Manning. Gqa: A new dataset for real-world visual reasoning and compositional question answering. In *Proceedings of the IEEE/CVF conference on computer vision and pattern recognition*, pages 6700–6709, 2019. 5, 7
- [29] Hamish Ivison, Akshita Bhagia, Yizhong Wang, Hannaneh Hajishirzi, and Matthew Peters. Hint: Hypernetwork instruction tuning for efficient zero-shot generalisation. *arXiv preprint arXiv:2212.10315*, 2022. 1, 2, 3
- [30] Max Jaderberg, Karen Simonyan, Andrea Vedaldi, and Andrew Zisserman. Synthetic data and artificial neural networks for natural scene text recognition. *arXiv preprint arXiv:1406.2227*, 2014. 5, 1
- [31] Chao Jia, Yinfei Yang, Ye Xia, Yi-Ting Chen, Zarana Parekh, Hieu Pham, Quoc Le, Yun-Hsuan Sung, Zhen Li, and Tom Duerig. Scaling up visual and vision-language representation learning with noisy text supervision. In *International conference on machine learning*, pages 4904–4916. PMLR, 2021. 1, 2
- [32] Lukasz Kaiser, Aidan N Gomez, Noam Shazeer, Ashish Vaswani, Niki Parmar, Llion Jones, and Jakob Uszkoreit. One model to learn them all. *arXiv preprint arXiv:1706.05137*, 2017. 3
- [33] Dimosthenis Karatzas, Faisal Shafait, Seiichi Uchida, Masakazu Iwamura, Lluís Gomez i Bigorda, Sergi Robles Mestre, Joan Mas, David Fernandez Mota, Jon Almazan Almazan, and Lluís Pere De Las Heras. Icdar 2013 robust reading competition. In *2013 12th international conference on document analysis and recognition*, pages 1484–1493. IEEE, 2013. 5, 6
- [34] Dimosthenis Karatzas, Lluís Gomez-Bigorda, Angelos Nicolaou, Suman Ghosh, Andrew Bagdanov, Masakazu Iwamura, Jiri Matas, Lukas Neumann, Vijay Ramaseshan Chandrasekhar, Shijian Lu, et al. Icdar 2015 competition on robust reading. In *2015 13th international conference on document analysis and recognition (ICDAR)*, pages 1156–1160. IEEE, 2015. 5, 6
- [35] Douwe Kiela, Alexis Conneau, Allan Jabri, and Maximilian Nickel. Learning visually grounded sentence representations. *arXiv preprint arXiv:1707.06320*, 2017. 3
- [36] Alex Krizhevsky, Geoffrey Hinton, et al. Learning multiple layers of features from tiny images. 2009. 5, 6
- [37] Dmitry Lepikhin, HyoukJoong Lee, Yuanzhong Xu, Dehao Chen, Orhan Firat, Yanping Huang, Maxim Krikun, Noam Shazeer, and Zhifeng Chen. Gshard: Scaling giant models with conditional computation and automatic sharding. *arXiv preprint arXiv:2006.16668*, 2020. 2
- [38] Hao Li, Jinguo Zhu, Xiaohu Jiang, Xizhou Zhu, Hongsheng Li, Chun Yuan, Xiaohua Wang, Yu Qiao, Xiaogang Wang, Wenhai Wang, et al. Uni-perceiver v2: A generalist model for large-scale vision and vision-language tasks. In *Proceedings of the IEEE/CVF Conference on Computer Vision and Pattern Recognition*, pages 2691–2700, 2023. 2, 3
- [39] Junnan Li, Dongxu Li, Silvio Savarese, and Steven Hoi. Blip-2: Bootstrapping language-image pre-training with frozen image encoders and large language models. *arXiv preprint arXiv:2301.12597*, 2023. 2, 7
- [40] Lei Li, Yuwei Yin, Shicheng Li, Liang Chen, Peiyi Wang, Shuhuai Ren, Mukai Li, Yazheng Yang, Jingjing Xu, Xu Sun, et al. M³it: A large-scale dataset towards multimodal multilingual instruction tuning. *arXiv preprint arXiv:2306.04387*, 2023. 2, 5, 6, 1
- [41] Liunian Harold Li, Pengchuan Zhang, Haotian Zhang, Jianwei Yang, Chunyuan Li, Yiwu Zhong, Lijuan Wang, Lu Yuan, Lei Zhang, Jenq-Neng Hwang, et al. Grounded language-image pre-training. In *Proceedings of the IEEE/CVF Conference on Computer Vision and Pattern Recognition*, pages 10965–10975, 2022. 1, 2
- [42] Tsung-Yi Lin, Michael Maire, Serge Belongie, James Hays, Pietro Perona, Deva Ramanan, Piotr Dollár, and C Lawrence Zitnick. Microsoft coco: Common objects in context. In *Computer Vision—ECCV 2014: 13th European Conference, Zurich, Switzerland, September 6–12, 2014, Proceedings, Part V 13*, pages 740–755. Springer, 2014. 2, 3, 1
- [43] Haotian Liu, Chunyuan Li, Qingyang Wu, and Yong Jae Lee. Visual instruction tuning. *arXiv preprint arXiv:2304.08485*, 2023. 3
- [44] Pengfei Liu, Xipeng Qiu, and Xuanjing Huang. Adversarial multi-task learning for text classification. *arXiv preprint arXiv:1704.05742*, 2017. 3
- [45] Xiaodong Liu, Pengcheng He, Weizhu Chen, and Jianfeng Gao. Multi-task deep neural networks for natural language understanding. *arXiv preprint arXiv:1901.11504*, 2019. 3
- [46] Shayne Longpre, Le Hou, Tu Vu, Albert Webson, Hyung Won Chung, Yi Tay, Denny Zhou, Quoc V Le, Barret Zoph, Jason Wei, et al. The flan collection: Designing data and methods for effective instruction tuning. *arXiv preprint arXiv:2301.13688*, 2023. 1, 2
- [47] Ilya Loshchilov and Frank Hutter. Decoupled weight decay regularization. *arXiv preprint arXiv:1711.05101*, 2017. 5
- [48] Simon M Lucas, Alex Panaretos, Luis Sosa, Anthony Tang, Shirley Wong, Robert Young, Kazuki Ashida, Hiroki Nagai,

- Masayuki Okamoto, Hiroaki Yamamoto, et al. Icdar 2003 robust reading competitions: entries, results, and future directions. *International Journal of Document Analysis and Recognition (IJ DAR)*, 7:105–122, 2005. [5](#), [6](#), [1](#)
- [49] Kenneth Marino, Mohammad Rastegari, Ali Farhadi, and Roozbeh Mottaghi. Ok-vqa: A visual question answering benchmark requiring external knowledge. In *Proceedings of the IEEE/cvf conference on computer vision and pattern recognition*, pages 3195–3204, 2019. [5](#), [7](#), [1](#)
- [50] Anand Mishra, Karteek Alahari, and CV Jawahar. Scene text recognition using higher order language priors. In *BMVC-British machine vision conference*. BMVA, 2012. [5](#), [6](#), [1](#)
- [51] Maxime Oquab, Timothée Darcet, Théo Moutakanni, Huy Vo, Marc Szafraniec, Vasil Khalidov, Pierre Fernandez, Daniel Haziza, Francisco Massa, Alaaeldin El-Nouby, et al. Dinov2: Learning robust visual features without supervision. *arXiv preprint arXiv:2304.07193*, 2023. [1](#), [2](#)
- [52] Adam Paszke, Sam Gross, Francisco Massa, Adam Lerer, James Bradbury, Gregory Chanan, Trevor Killeen, Zeming Lin, Natalia Gimelshein, Luca Antiga, et al. Pytorch: An imperative style, high-performance deep learning library. *Advances in neural information processing systems*, 32, 2019. [5](#)
- [53] Zhiliang Peng, Li Dong, Hangbo Bao, Qixiang Ye, and Furu Wei. Beit v2: Masked image modeling with vector-quantized visual tokenizers. *arXiv preprint arXiv:2208.06366*, 2022. [2](#)
- [54] Trung Quy Phan, Palaiahnakote Shivakumara, Shangxuan Tian, and Chew Lim Tan. Recognizing text with perspective distortion in natural scenes. In *Proceedings of the IEEE international conference on computer vision*, pages 569–576, 2013. [5](#), [6](#)
- [55] Bryan A Plummer, Liwei Wang, Chris M Cervantes, Juan C Caicedo, Julia Hockenmaier, and Svetlana Lazebnik. Flickr30k entities: Collecting region-to-phrase correspondences for richer image-to-sentence models. In *Proceedings of the IEEE international conference on computer vision*, pages 2641–2649, 2015. [5](#), [1](#)
- [56] Subhojeet Pramanik, Priyanka Agrawal, and Aman Hussain. Omnet: A unified architecture for multi-modal multi-task learning. *arXiv preprint arXiv:1907.07804*, 2019. [3](#)
- [57] Alec Radford, Jong Wook Kim, Chris Hallacy, Aditya Ramesh, Gabriel Goh, Sandhini Agarwal, Girish Sastry, Amanda Askell, Pamela Mishkin, Jack Clark, et al. Learning transferable visual models from natural language supervision. In *International conference on machine learning*, pages 8748–8763. PMLR, 2021. [1](#), [2](#), [3](#)
- [58] Samyam Rajbhandari, Jeff Rasley, Olatunji Ruwase, and Yuxiong He. Zero: Memory optimizations toward training trillion parameter models. In *SC20: International Conference for High Performance Computing, Networking, Storage and Analysis*, pages 1–16. IEEE, 2020. [5](#)
- [59] Victor Sanh, Thomas Wolf, and Sebastian Ruder. A hierarchical multi-task approach for learning embeddings from semantic tasks. In *Proceedings of the AAAI Conference on Artificial Intelligence*, pages 6949–6956, 2019. [3](#)
- [60] Victor Sanh, Albert Webson, Colin Raffel, Stephen H Bach, Lintang Sutawika, Zaid Alyafeai, Antoine Chaffin, Arnaud Stiegler, Teven Le Scao, Arun Raja, et al. Multi-task prompted training enables zero-shot task generalization. *arXiv preprint arXiv:2110.08207*, 2021. [1](#), [2](#)
- [61] Anders Søgaard and Yoav Goldberg. Deep multi-task learning with low level tasks supervised at lower layers. In *Proceedings of the 54th Annual Meeting of the Association for Computational Linguistics (Volume 2: Short Papers)*, pages 231–235, 2016. [3](#)
- [62] Johannes Stalkamp, Marc Schlipf, Jan Salmen, and Christian Igel. Man vs. computer: Benchmarking machine learning algorithms for traffic sign recognition. *Neural networks*, 32:323–332, 2012. [5](#), [6](#)
- [63] Trevor Standley, Amir Zamir, Dawn Chen, Leonidas Guibas, Jitendra Malik, and Silvio Savarese. Which tasks should be learned together in multi-task learning? In *International Conference on Machine Learning*, pages 9120–9132. PMLR, 2020. [3](#)
- [64] Gjorgji Strezoski, Nanne van Noord, and Marcel Worring. Many task learning with task routing. In *Proceedings of the IEEE/CVF International Conference on Computer Vision*, pages 1375–1384, 2019. [3](#)
- [65] Chen Sun, Abhinav Shrivastava, Saurabh Singh, and Abhinav Gupta. Revisiting unreasonable effectiveness of data in deep learning era. In *Proceedings of the IEEE international conference on computer vision*, pages 843–852, 2017. [2](#)
- [66] Quan Sun, Yuxin Fang, Ledell Wu, Xinlong Wang, and Yue Cao. Eva-clip: Improved training techniques for clip at scale. *arXiv preprint arXiv:2303.15389*, 2023. [1](#), [2](#), [3](#), [6](#), [7](#)
- [67] Hugo Touvron, Matthieu Cord, Matthijs Douze, Francisco Massa, Alexandre Sablayrolles, and Hervé Jégou. Training data-efficient image transformers & distillation through attention. In *International conference on machine learning*, pages 10347–10357. PMLR, 2021. [1](#)
- [68] Hugo Touvron, Thibaut Lavril, Gautier Izacard, Xavier Martinet, Marie-Anne Lachaux, Timothée Lacroix, Baptiste Rozière, Naman Goyal, Eric Hambro, Faisal Azhar, et al. Llama: Open and efficient foundation language models. *arXiv preprint arXiv:2302.13971*, 2023. [3](#)
- [69] Haohan Wang, Songwei Ge, Zachary Lipton, and Eric P Xing. Learning robust global representations by penalizing local predictive power. *Advances in Neural Information Processing Systems*, 32, 2019. [5](#), [6](#), [1](#)
- [70] Kai Wang, Boris Babenko, and Serge Belongie. End-to-end scene text recognition. In *2011 International conference on computer vision*, pages 1457–1464. IEEE, 2011. [5](#), [6](#)
- [71] Yizhong Wang, Yeganeh Kordi, Swaroop Mishra, Alisa Liu, Noah A Smith, Daniel Khashabi, and Hannaneh Hajishirzi. Self-instruct: Aligning language model with self generated instructions. *arXiv preprint arXiv:2212.10560*, 2022. [2](#)
- [72] Jason Wei, Maarten Bosma, Vincent Y Zhao, Kelvin Guu, Adams Wei Yu, Brian Lester, Nan Du, Andrew M Dai, and Quoc V Le. Finetuned language models are zero-shot learners. *arXiv preprint arXiv:2109.01652*, 2021. [1](#), [2](#), [8](#)
- [73] Kelvin Xu, Jimmy Ba, Ryan Kiros, Kyunghyun Cho, Aaron Courville, Ruslan Salakhudinov, Rich Zemel, and Yoshua Bengio. Show, attend and tell: Neural image caption generation with visual attention. In *International conference on machine learning*, pages 2048–2057. PMLR, 2015. [4](#), [5](#)

- [74] Zhiyang Xu, Ying Shen, and Lifu Huang. Multiinstruct: Improving multi-modal zero-shot learning via instruction tuning. *arXiv preprint arXiv:2212.10773*, 2022. 3
- [75] F Xue, Z Zheng, and Y You. Instruction in the wild: A user-based instruction dataset, 2023. 2
- [76] Hanrong Ye and Dan Xu. Inverted pyramid multi-task transformer for dense scene understanding. In *European Conference on Computer Vision*, pages 514–530. Springer, 2022. 2, 3
- [77] Hanrong Ye and Dan Xu. Taskprompter: Spatial-channel multi-task prompting for dense scene understanding. In *The Eleventh International Conference on Learning Representations*, 2022. 2, 3
- [78] Jiahui Yu, Zirui Wang, Vijay Vasudevan, Legg Yeung, Mojtaba Seyedhosseini, and Yonghui Wu. Coca: Contrastive captioners are image-text foundation models. *arXiv preprint arXiv:2205.01917*, 2022. 2
- [79] Amir R Zamir, Alexander Sax, William Shen, Leonidas J Guibas, Jitendra Malik, and Silvio Savarese. Taskonomy: Disentangling task transfer learning. In *Proceedings of the IEEE conference on computer vision and pattern recognition*, pages 3712–3722, 2018. 3
- [80] Amir R Zamir, Alexander Sax, Nikhil Cheerla, Rohan Suri, Zhangjie Cao, Jitendra Malik, and Leonidas J Guibas. Robust learning through cross-task consistency. In *Proceedings of the IEEE/CVF Conference on Computer Vision and Pattern Recognition*, pages 11197–11206, 2020. 3
- [81] Bo Zhao, Boya Wu, and Tiejun Huang. Svit: Scaling up visual instruction tuning. *arXiv preprint arXiv:2307.04087*, 2023. 3
- [82] Yiwu Zhong, Jianwei Yang, Pengchuan Zhang, Chunyuan Li, Noel Codella, Liunian Harold Li, Luwei Zhou, Xiyang Dai, Lu Yuan, Yin Li, et al. Regionclip: Region-based language-image pretraining. In *Proceedings of the IEEE/CVF Conference on Computer Vision and Pattern Recognition*, pages 16793–16803, 2022. 1, 2
- [83] Chunting Zhou, Pengfei Liu, Puxin Xu, Srini Iyer, Jiao Sun, Yuning Mao, Xuezhe Ma, Avia Efrat, Ping Yu, Lili Yu, et al. Lima: Less is more for alignment. *arXiv preprint arXiv:2305.11206*, 2023. 1, 2
- [84] Jinguo Zhu, Xizhou Zhu, Wenhai Wang, Xiaohua Wang, Hongsheng Li, Xiaogang Wang, and Jifeng Dai. Uni-perceiver-moe: Learning sparse generalist models with conditional moes. *Advances in Neural Information Processing Systems*, 35:2664–2678, 2022. 2, 3

Supervised Fine-tuning *in turn* Improves Visual Foundation Models

Supplementary Material

A. ViSFT Procedure

The ViSFT training process can be described in Algorithm 1 and Algorithm 2, which obtain compatible in-domain task head T_n^* and learned LoRA weights ΔW^* , respectively.

Upon acquiring the learned LoRA weights ΔW^* , evaluations on out-of-domain benchmarks can be outlined in Algorithm 3.

Algorithm 1 Stage1 Training

Require: Training dataset $D(\mathbf{x}, \mathbf{y})$; Pretrained vision foundation model M

- 1: Initialize an in-domain task head T_n , for $n \in \{1, \dots, N\}$ and freeze M
- 2: **for** $i = 1, 2, \dots$ **do** ▷ Can be executed in parallel
- 3: Extract feature $\mathbf{f} = M(\mathbf{x})$ for input \mathbf{x}
- 4: Minimize $L_n(\mathbf{y}, T_n(\mathbf{f}))$ on D to obtain T_n^*
- 5: **end for**

Algorithm 2 Stage2 Training

Require: In-domain task head T_n^* ; Pretrained vision foundation model M ; Sampling probability α_n , $n \in \{1, \dots, N\}$

- 1: Initialize LoRA weights ΔW , freeze M and T_n^* , $n \in \{1, \dots, N\}$
- 2: **for** $i = 1, 2, \dots$ **do**
- 3: Select an in-domain task T_n^* according to $P(\alpha_n)$
- 4: Extract feature $\mathbf{f}' = M(\mathbf{x}; \Delta W)$ for input \mathbf{x}
- 5: Minimize $L_n(\mathbf{y}, T_n(\mathbf{f}'))$ on D to obtain ΔW^*
- 6: **end for**

Algorithm 3 Evaluation

Require: Pretrained vision foundation model M ; Learned LoRA weights ΔW^* ; Out-of-domain benchmark T_o ; Evaluation dataset $E_o(\mathbf{x}, \mathbf{y})$, $o \in \{1, \dots, O\}$

- 1: Initialize results list R_o
- 2: **for** \mathbf{x} in $E_o(\mathbf{x})$ **do**
- 3: Extract feature $\mathbf{f}^* = M(\mathbf{x}; \Delta W^*)$ for input \mathbf{x}
- 4: Predicting $R_o = [R_o, T_o(\mathbf{f}^*)]$
- 5: **end for**
- 6: Accumulate results: $Metric(E_o(\mathbf{y}), R_o)$ on E_o

B. Licenses of Datasets

ImageNet-1k [11] is subject to the ImageNet terms of use [99].

ImageNet-A [25] is subject to the ImageNet-A terms of use [88].

ImageNet-R [24] is subject to the ImageNet-R terms of use [89].

ImageNet-Sketch [69] is subject to the ImageNet-Sketch terms of use [90].

EuroSAT [23] is subject to the EuroSAT terms of use [86].

Caltech-101 [16] is subject to the Caltech-101 terms of use [94].

IC03 [48] is subject to the ICDAR 2003 terms of use [96].

IIIT [50] is subject to the IIIT5k-word terms of use [87].

MJSynth [30] is subject to the MJSynth terms of use [97].

SynthText [19] is subject to the SynthText terms of use [98].

M³IT [40] is subject to the M³IT terms of use [91].

COCO [42] is subject to the COCO terms of use [85].

Flickr30K [55] is subject to the Flickr terms of use [95].

VQAv2 [18] is subject to the VQAv2 terms of use [92].

OK-VQA [49] is subject to the OK-VQA terms of use [93].

Appendix References

- [85] Coco terms & conditions of use. <https://cocodataset.org/#termsofuse>.
- [86] Eurosat terms & conditions of use. <https://github.com/pheelber/EuroSAT/blob/master/LICENSE>.
- [87] Iiit5k-word terms & conditions of use. <https://cvit.iiit.ac.in/images/Projects/SceneTextUnderstanding/IIIT5Kfiles/README.txt>.
- [88] Imagenet-a terms & conditions of use. <https://github.com/hendrycks/natural-adv-examples/blob/master/LICENSE>.
- [89] Imagenet-r terms & conditions of use. <https://github.com/hendrycks/imagenet-r/blob/master/LICENSE>.
- [90] Imagenet-sketch terms & conditions of use. <https://github.com/HaohanWang/ImageNet-Sketch/blob/master/LICENSE>.
- [91] M³it terms & conditions of use. <https://huggingface.co/datasets/MMInstruction/M3IT-80>.
- [92] Vqav2 terms & conditions of use. <https://visualqa.org/terms.html>.
- [93] AllenAI. Ok-vqa terms & conditions of use. <https://allenai.org/terms>.
- [94] Lab. Caltech. Caltechdata terms & conditions of use. <https://library.caltech.edu/search/caltechdata#terms>.
- [95] Inc. Flickr. Flickr terms & conditions of use. <https://www.flickr.com/help/terms>.
- [96] Hideaki Goto. Icdar 2003 terms & conditions of use. <http://www.imglab.org/db/files/README-ICDAR2003-SceneTrainTrain-GT4.txt>.
- [97] Oxford. Mjsynth terms & conditions of use. <https://www.robots.ox.ac.uk/~vgg/data/text/#sec-synth>.
- [98] Oxford. Synthtext terms & conditions of use. <https://www.robots.ox.ac.uk/~vgg/terms/dataset-group-2-access.html>.
- [99] Princeton University and Stanford University. Imagenet terms & conditions of use. <https://image-net.org/download>.